Int. J. Electrochem. Sci., 13 **(2018)** 11443 – 11453, doi: 10.20964/2018.12.67

International Journal of
ELECTROCHEMICAL
SCIENCE
www.electrochemsci.org

Confine Sulfur in Mesoporous Chromium-Metal–Organic Frameworks (MIL-101) for Long-life Lithium–Sulfur Batteries

Wenxiao Su[2], Wangjun Feng [1,2,], Guangjie Gao[2], Lijing Chen[2], Miaomiao Li, Changkun Song[2],*

[1] State Key Laboratory of Advanced Processing and Recycling Nonferrous Metals, Lanzhou University of Technology, Lanzhou 730050, China;
[2] School of Science, Lanzhou University of Technology, Lanzhou 730050, China)
[*]E-mail: wjfeng@lut.cn

Received: 3 September 2018 / *Accepted:* 23 September 2018 / *Published:* 5 November 2018

Large surface area and mesoporous Chromium-Metal–Organic Frameworks (MIL-101(Cr)) have been prepared as a sulfur host for long-life Li-S batteries. The MIL-101(Cr)/S cathode exhibits excellent electrochemical performance, high initial discharge capacity of 1210.5 mAh g^{-1} at 0.1 C and a retentive capacity of 60.1% after 400 cycles at 0.2 C. Especially, the capacity contributed by the first platform of the discharge is only attenuated by 66.71mA g^{-1} at the current density of from 0.1C increasing to 0.5C, which means that MIL-101(Cr)/S can obviously inhibit the occurrence of the shuttle effect. Experimental results indicate that the MIL-101(Cr) is a potential host material for the long-life and high performance lithium–sulfur batteries.

Keywords: MIL-101(Cr); Lithium-sulfur battery; Sulfur cathode; Shuttle effect.

1. INTRODUCTION

In recent years, ever-increasing research have attracted in advanced materials for Li-ion batteries to tackle the demand of energy storage. The Li–S battery is widely recognized as a promising next-generation commercial energy storage devices based on the high theoretical capacity (1672mAh g^{-1}), the low-cost of sulfur, and the environmental benignity [1]. Nevertheless, the practical applications of Li−S batteries exist some critical challenges. Firstly, the low ion and electron conductivity nature of sulfur and its reduction products (Li_2S_2 and Li_2S) result in slow electrochemical reaction kinetic and low utilization of sulfur in charge and discharge. Secondly, the main problem of Li-S battery is the dissolution of polysulfides in organic electrolyte forming the shuttle effect between the electrodes during the electrochemical reaction, which lead to the low Coulombic efficiency and loss of active materials. Furthermore, the product of polysulfides react with anode of lithium metal will

deposited on the surface of lithium anode, causing the deactivation of Li anode. These serious issues bring about unstable electrochemical performance and a rapid fading of capacity [2].

Extensive research efforts have been made to address the intractable problems about Li–S batteries. Using cellular structure carbon materials as the host of sulfur is the most popular method because its better electrical conductivity not only facilitate the Li-ions and electrons transfer during charge and discharge, but also help to trap polysulfides through physisorption. Graphene and reduced graphene oxide [3-6], carbon nanotubes [7 8], three-dimensional (3D) Graphene-carbon nanotube (CNT)
composites [9], and porous carbon [10-12] because of its large surface area, excellent conductivity and pore volume have been employed as the host for sulfur to improve the conductivity and slow the shuttle effect of the polysulfides on the cathode. Those C-S composites using the cathode materials exhibit excellent electrochemical performance and cycle stability. Nonetheless, the adsorption force between the porous carbon and polysulfides is the relatively weak van der Waals force, which does not trap high polar lithium polysulfides strongly. Therefore, in order to suppress the shuttle effect of polysulfides optimally by stronger chemisorption, $Mg_{0.6}Ni_{0.4}O$ [13], MoO_2 [14], Ti_4O_7 [15], TiO_2 [16], MnO_2 [17], metal-like TiC [18], and CoS_2[19] polar compounds have served as hosts for polysulfide adsorption and proved that some metal oxides and metal sulfide show strong chemical interactions between sulfur species and metals metal oxides or sulfide resulting in the enhanced electrochemical performance for Li–S batteries. Even so, the introduction of metal oxides and metal sulfide in the cathode obviously reduced the content of sulfur on unit area cathode.

Metal organic frameworks (MOFs), can be composed of metal ions and organic ligands hybrid porous materials. MOFs were extensively studied as gas adsorbents, gas storage, catalyst materials and sensors attribute to their plentiful pore, extra specific surface area, and tunable opening [20]. Specifically, Co-based ZIF-67[21], Cu-based HKUST-1[22] have been chosen as carrier of sulfur to confine shuttle effect about polysulfides through both the physical adsorption of porous structure and chemical interaction between metal atoms and polysulfides for Li-S battery. Those strategies put forward a new way to suppressed polysulfides and improved electrochemical performance for Li-S battery. In this paper, we choose MIL-101(Cr) as the sulfur host because of its much larger surface area (1919.7m^2g^{-1}) and pore volume (1.06 cm^3 g^{-1}), which can provide abundant channels and cavities with an average pore diameter of 2.29 nm. The unique pore structure and high surface area would contribute to the high dispersion of sulfur into the pores. The prepared MIL-101(Cr)/S composite as the cathode for Li-S battery possesses a much better specific capacity and good cycle performance which mainly results from the capturing ability of MIL-101 for polysulfides.

2. EXPERIMENTAL

2.1. Preparation of the Chromium-Metal–Organic Frameworks (MIL-101(Cr))

The MIL-101(Cr) was prepared by simple hydrothermal reaction method. Typically, 0.996 g terephthalic acid and 2.4 g Cr $(NO_3)_3 9H_2O$ were poured into the 30mL ultrapure water and stirred 30 minutes. Then, 0.1ml hydrofluoric acid was put into mixed solution and transferred to a 60mL Teflon-

lined stainless bomb and kept 220°C for 8h. In order to thoroughly remove the unreacted terephthalic acid from the cavities of MIL-101(Cr), the filter residue was transferred to a 60mL Teflon-lined stainless bomb and kept 120°C for 8h. After cooling down, the crystallized green powder was further purified by alternate washing with deionized water, DMF, and ethanol. Finally, the MIL-101(Cr) was collected via centrifugation at 4000 rpm for 30 min and dry under vacuum at 60 °C for 12 h.

2.1. Preparation of the MIL-101(Cr)/S cathode.

The MIL-101(Cr)/S composite were prepared by the traditional melt diffusion technique. Typically, the prepared MIL-101(Cr) and sublimed sulfur were ground together for 20 min at a mass ratio of 3:7 and put into 50-mL Teflon-lined stainless-steel bomb keeping at a temperature of 155°C for 20 h. Finally, the final MIL-101(Cr)/S composites were obtained.

To prepare the electrode, the MIL-101(Cr)/S composite, super P, and polyvinylidene fluoride (PVDF) at a weight ratio of 7:2:1 mixed together and stirred for 20 h in vials with N-methyl-2-pyrrolidone (NMP) as the solvent. Then, the mixed slurry was evenly coated on the Al foil and dried at 55 °C for 12 h in vacuum obtaining the cathode film. The prepared cathode film was punched into 9-mm diameter discs. The loading of the active material was approximately 1–2 mg cm^{-2} on every cathode plate.

2.2 Materials characterization

The phase of all the samples were analysed by X-ray diffraction (XRD) using a Bruker D8 Advance diffractometer with Cu Kα radiation from 5º to 80º (Rigaku Corporation Tokyo, Japan). The surface images of the MIL-101(Cr) and MIL-101(Cr)/S cathode were taken using scanning electron microscopy (SEM; JSM-6700F, JEOL, Tokyo, Japan) at 20 kV. The total pore volumes, specific surface area and pore size distribution were estimated by Brunauer-Emmett-Teller (BET) methods. The sulfur content of composites were measured using thermogravimetric analysis (TGA; STA449C, NETZSCH, Germany).

2.2 Electrochemical characterization

The electrochemical performances of the MIL-101(Cr)/S composites were tested by assembling CR2025 coin cells. The Celgard 2400 and 15.8 mm lithium foil serve as the separator and counter electrodes, respectively. The electrolyte was composed of 1M lithium hexafluorophosphate (LiTFSI) 1,3-dioxolane (DOL) and DME (1:1 by volume) with 2 wt% $LiNO_3$ as the additive. 20 μL of electrolytes per gram of sulfur were added to each cell. The charge-discharge performances were tested by LAND-CT2001A battery test instruments (Wuhan Jinnuo, China) within a voltage range of 1.7 to 2.8 V (vs. Li/Li^+) at difference C rates (1 C = 1672 mA h g^{-1}). The CV measurements and were performed using the CS350 Electrochemical workstation (Corrtest Inc., Wuhan, China) within a range of 1.7-2.8 V at a scanning rate of 0.1 mV s^{-1}.

3. RESULTS AND DISCUSSION

3.1. Materials characterization

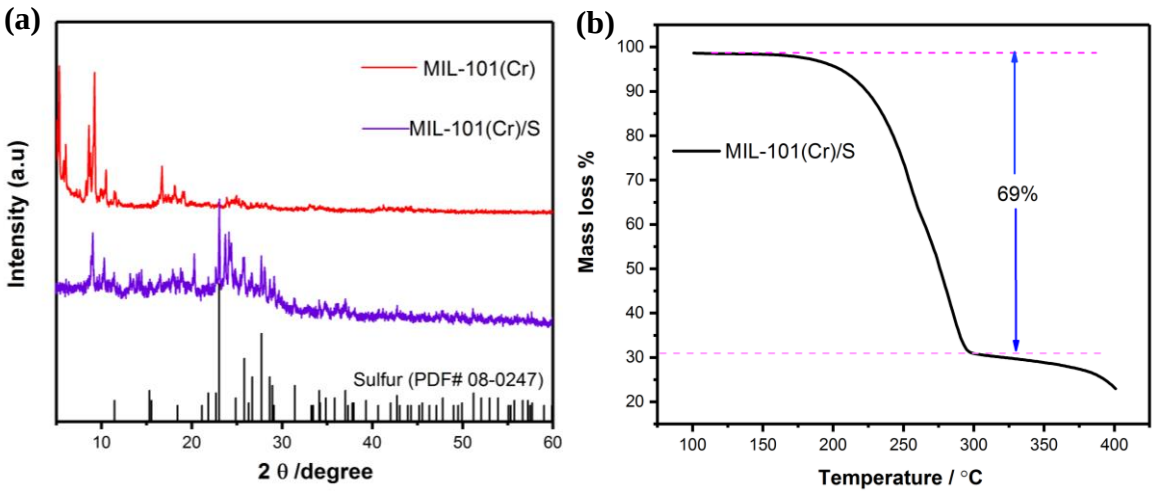

Figure 1. (a) X-ray diffraction patterns of sublimated sulfur, MIL-101(Cr) and MIL-101(Cr)/S composite; (b) TGA curve of the MIL-101(Cr)/S composite

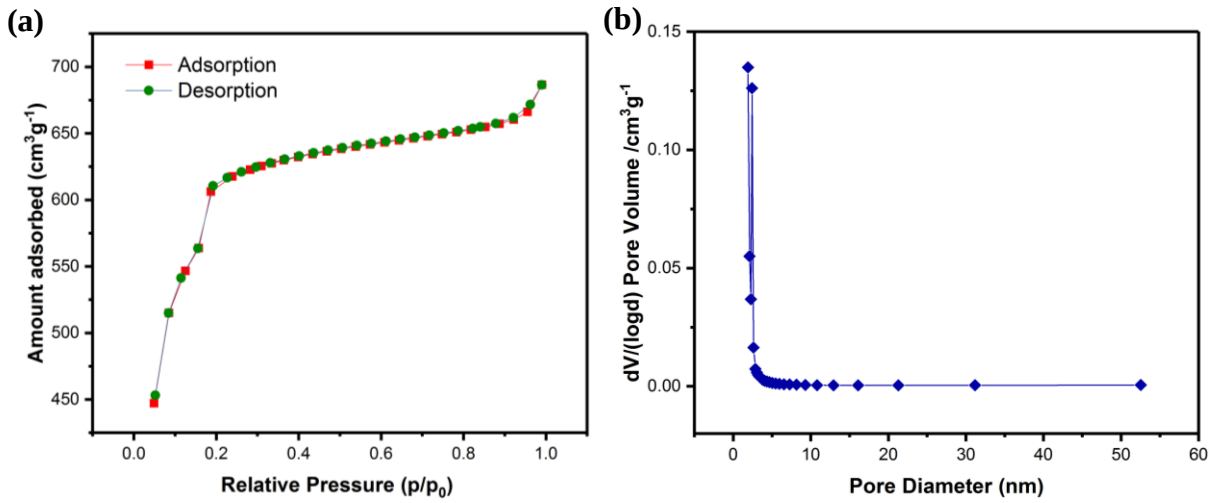

Figure 2. (a) N_2 adsorption–desorption isotherm curves from the MIL-101(Cr), (b) pore size distribution of the MIL-101(Cr),

The crystalline phase of MIL-101(Cr) and the MIL-101(Cr)/S composite were analyzed by X-Ray Diffraction (XRD). The XRD strong peaks and positions can be observed mainly at 5° to 20°, indicating the stability of the periodical structure of Cr-MIL-101. This is basically consistent with the previously published literature [23]. Combined with the XRD patterns of MIL-101(Cr), MIL-101(Cr)/S and standard patterns of sulfur (PDF#08-0247) found that the patterns of MIL-101(Cr)/S contained a strong peak of MIL-101(Cr) at 9° and all peaks of sulfur. This phenomenon indicates that

the sulfur has homogeneously distributed in the pores of MIL-101(Cr) rather than adhere on the surface of MIL-101(Cr).

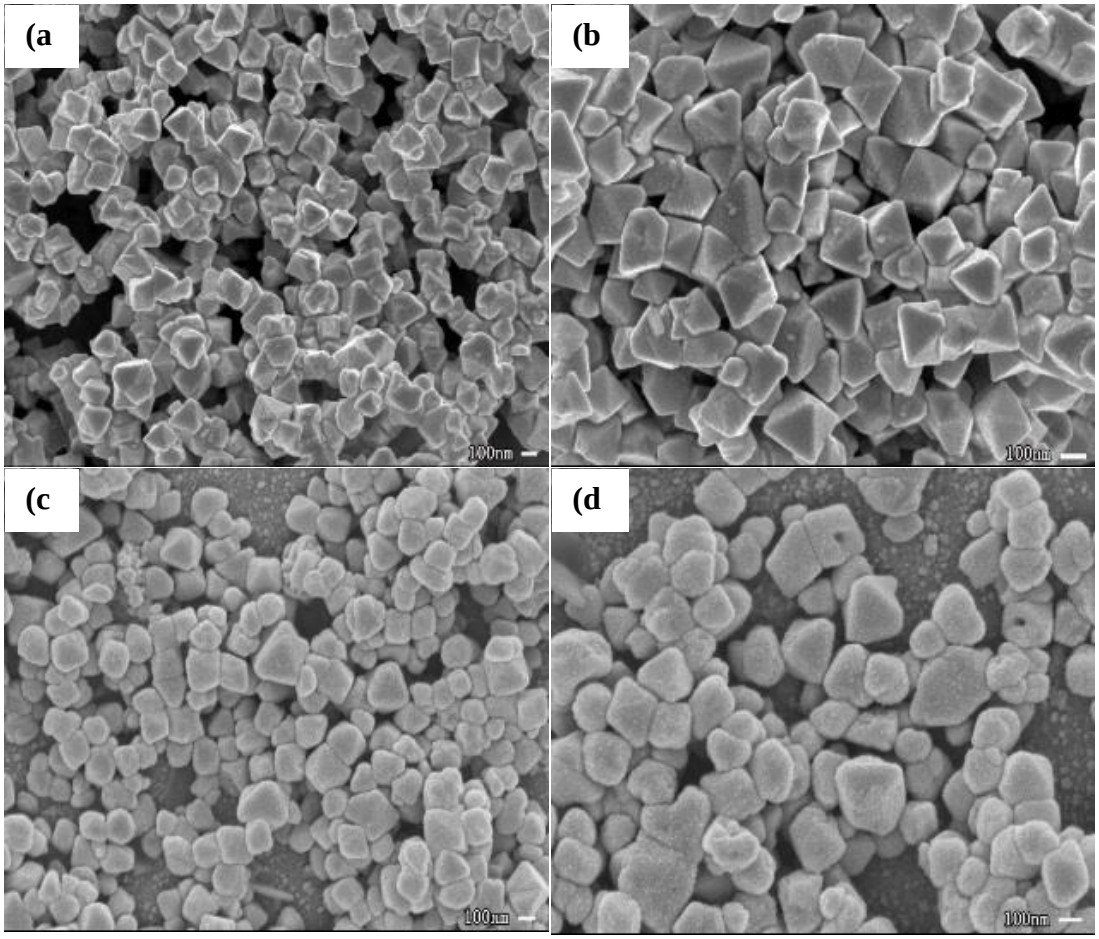

Figure 3. (a) (b) SEM images of MIL-101(Cr), (d) (e) SEM images of MIL-101(Cr)/S

N_2 adsorption and desorption measurements were employed to explore the internal porous structure of sample. As shown as Figure 2a, typical type I with a surface area of about 1261.7 $m^{2}{\cdot}g^{-1}$can be measured, and exhibit a surface area of 1919.7 m^2/g. Figure 2b shows the distribution of average pore diameter of MIL-101(Cr), calculating with the Barrett–Joyner–Halenda (BJH) method. The average pore diameter of MIL-101(Cr) is around 2.28 nm and a pore volume of 1.0617 cm^3/g, and similar with previously reported literature [24]

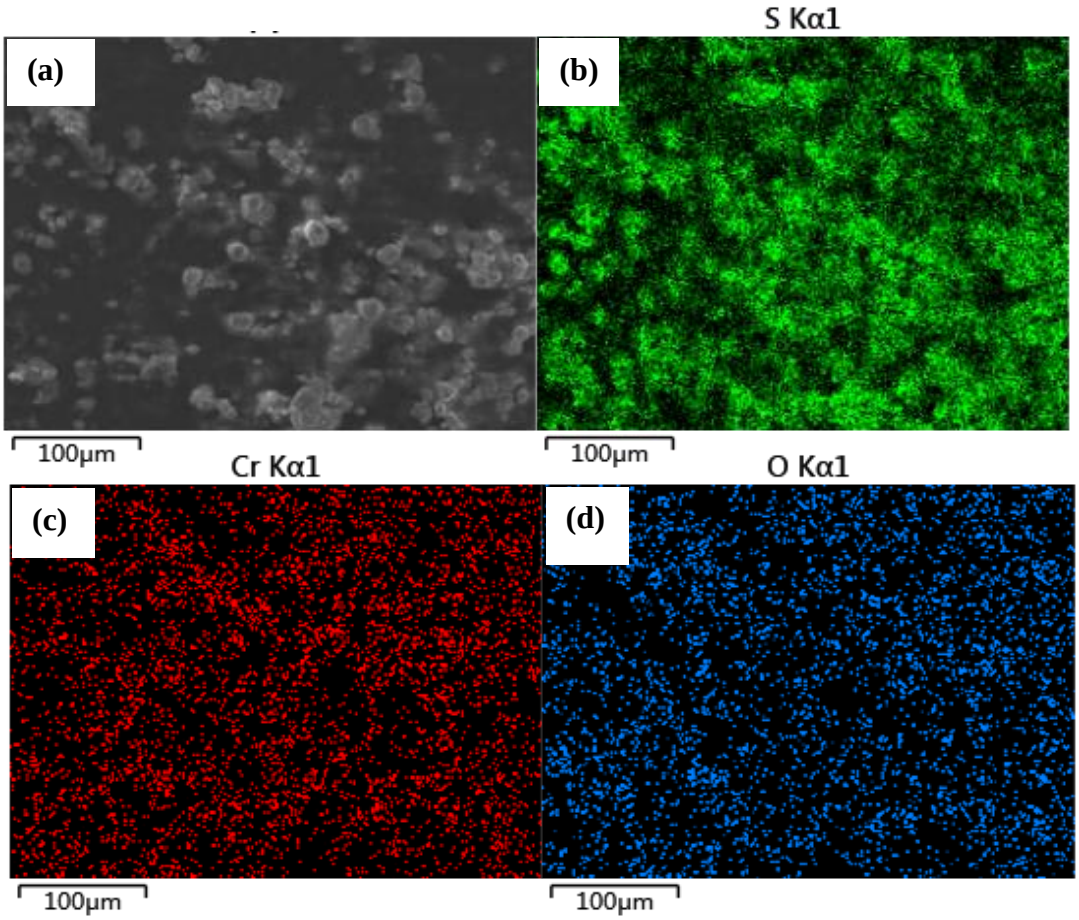

Figure 4. (a) SEM images of MIL-101(Cr); (b), (c), (d) EDS mappings showing the distribution of S, Cr and O;

The SEM images of the MIL-101(Cr) and MIL-101(Cr)/S composite are shown in Figure 3. From the Figure 3a and 3b, the MIL-101(Cr) crystals diameters are distinctly observed with 80–200 nm. The lattice structure of MIL-101(Cr) is the MTN-type hybrid structure with a trimer of metal octahedra chelated by two carboxylic functions [25]. As we all known, the nanocrystallization of material size will show many excellent mechanical optics and electrochemical properties [26]. Figure. 3c and 3d is the SEM images of MIL-101(Cr)/S composite. After a melt infiltration treatment at 155 °C for sulfur and MIL-101, the MIL-101(Cr)/S composite was still maintaining the shape of regular octahedron. Compare with the images of MIL-101 and MIL-101(Cr)/S composite, the difference is that the edge of MIL-101(Cr)/S becomes less sharp than MIL-101. Combined with the SEM mapping (Figure 4) of MIL-101(Cr)/S, we can speculate that the sulfur highly and uniformly dispersed in the pore of MIL-101(Cr), because there is 69% sublimed sulfur in the MIL-101(Cr)/S composite by TGA measurement (Figure 1 b), but no separate sulfur particles have been found in the SEM image and element distribution of the composite.

3.2 Electrochemical performance

The electrochemical performances of MIL-101(Cr)/S cathode were evaluated by the testing of charge and discharge at difference current density and hundreds of charge-discharge cycles at same current density. Figure 5. (a) shows the charge-discharge capacity curves of the initial cycles for the MIL-101(Cr)/S cathode at a rate current density of 0.1 C, 0.2, 0.5C, and 1C, respectively. It is obvious from the profile that two discharge plateaus are clearly shown in the curves at 0.1C, 0.2C, and 0.5C current density.

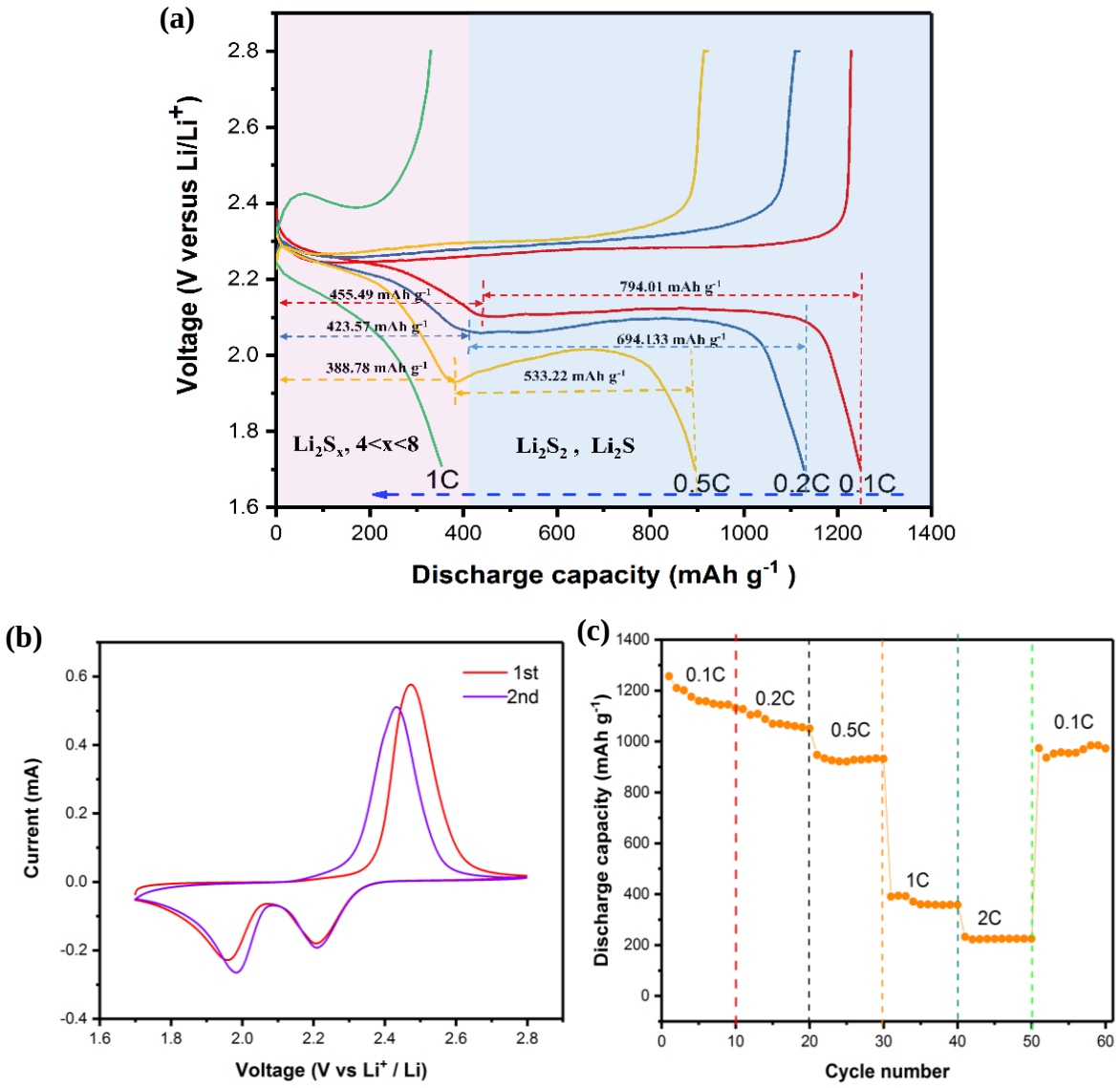

Figure 5. (a) Charge-discharge capacity curves of the initial cycles of the MIL-101(Cr)/S cathode at a rate current density of 0.1 C, 0.2, 0.5C, and 1C; (b) The initial two CV curves of the MIL-101(Cr)/S cathode at scanning rate of 0.1 mV s^{-1} (c) Rate capability of the MIL-101(Cr)/S

However, the second plateau disappeared at higher 1C current density. It is very clear that the first discharge plateau at 2.3V corresponds to the formation of sulfur to long-chain polysufides (Li_2S_x,

4<x<8), the second discharge plateau at 2.1V corresponds to the formation long-chain polysufides to insoluble short-chain Li_2S_2 and Li_2S [27]. The MIL-101(Cr)/S cathode delivers higher discharge specific capacity of 1249.5 mAh g^{-1}, 1117.7 mA h g^{-1} and 922 mA h g^{-1} at current density of 0.1C, 0.2C, and 0.5C, respectively. Nevertheless, the specific capacity is only 330.3 mA h g^{-1} and the second plateau disappeared at current density of 1C. This may be mainly due to the poor conductivity of the internal structure of MIL-101(Cr), which result in the slow electrochemical reaction kinetics of the transformation of liquid phase Li_2S_x (4<x<8) to the solid phase Li_2S_2 and Li_2S during the charge and discharge. Significantly, with the increasing of current density from 0.1C to 0.5C, although the discharge specific capacity contributed by the second plateau at 2.1 V decays rapidly from 1249.5 mA h g^{-1} to 922 mA h g^{-1}, the discharge specific capacity contributed by the first platform at 2.3V is only attenuated 66.71mA h g^{-1}. Compared with other sulfur host for Li-S batteries, MI-101(Cr) exhibit higher capacity contributions at first charge-discharge plateau (Table1). According to the electronic gain and loss calculation, the first discharge plateau can provide the 419 mAh g^{-1} theoretical capacity, and the second discharge plateau can provide 1256 mAh g^{-1} theoretical capacity. From the Table1, When the carbon material is used as a carrier of sulfur, the first discharge platform exhibits a lower capacity, mainly because non-polar carbon is insufficient to adsorb polysulfide. Excessive metal sulfides exhibit higher capacity due to stronger polar chemical adsorption of lithium polysulfide [28]. MIL-101(Cr)/S cathode shows the closed theoretical capacity at the first discharge platform, but the capacity contributed at the second platform is not as good as other porous carbon materials[2, 9, 30]. This interesting phenomenon imply that the main problem of MIL-101(Cr) as a host of sulfur is that the difficulty of transformation during lithium polysulfide and Li_2S, but its rich pore structure and large surface area have great advantages to suppressing the shuttle effect of polysulfides. Therefore, this phenomenon reveals the huge application potential of MIL-101(Cr) in lithium-sulfur batteries. If some strategies are used to improve the conductivity for MIL-101(Cr), we believe that MIL-101(Cr) will be able to better serve lithium-sulfur batteries.

In order to reveal the electrochemical processes and electrochemical kinetics of MIL-101(Cr)/S cathode during charge- discharge. Cyclic voltammogram (CV) curves are tested within the potential range of 1.7 and 2.8 V at scanning rate of 0.1 mV s^{-1}. The initial two CV curves of MIL-101(Cr)/S cathode are shown in Figure 5b. As shown as the curves in the first two cycles, an oxidation peak and two reduction peaks can be observed. The reduction peaks at 2.3V correspond to the lithiation reactions of sulfur rings (S8) to long-chain lithium polysulfides (Li_2S_n, 4≤n<8), and the second reduction peak at 2.07 V is related to the further reduction of lithium polysulfides to electrolyte-insoluble Li_2S_2 and Li_2S [1]. This is consistent with the two discharge plateaus. It can be seen that the oxidation peak is obviously shifted to higher voltage from the first cycle to the second cycle. This shift reveals that the electrochemical reactions need to overcome the strong energy absorption between S and the host matrix [29].

The MIL-101(Cr)/S cathode is tested at different current densities to study the rate capability performance. As shown as Figure 5c, a specific capacity of 1210.5, 1127.6, 947.7, 390.2, and 232.3 mA h g^{-1} can be obtained at 0.1C, 0.2C, 0.5C, 1C and 2C current density, respectively. Obviously, the capacity of the MIL-101(Cr)/S cathode decreases gradually from the reversible 1210.5 mA h g^{-1}at 0.1 C to 947.7, at 1210.5 mA h g^{-1} at 0.5C. However, the capacity of the MIL-101/S cathode decreases

rapidly from the 947.7 mA h g^{-1}at 0.5 C to 232.3 mA h g^{-1} at 2C. Combined with the analysis of charge-discharge capacity curves of the initial cycles, we can make a conclusion that MIL-101(Cr) as a host of sulfur can effectively inhibit the shuttle effect of lithium polysulfides, but its poor conductivity limits the charging and discharging of large currents density for Li-S batteries. The main reason maybe is that the sulfur of inside in the pores cannot be fully reaction with the higher current density. When the charge and discharge current density returned to 0.1C, the capacity can retain back to 973.6 mA h g^{-1}, showing a good rate capability at low current density.

Host of sulfur	The capacity of first plateau at 0.5C (mAh g^{-1})	The capacity of second plateau at 0.5C(mAh g^{-1})	Ref
N,S-codoped graphene	280	520	[2]
3D Graphene Nanosheet@Carbon	210	490	[9]
Honeycomb-like Co@N−C Composite	220	680	[30]
RGO@ZIF67	200	590	[31]
MoS2 nanoflakes	350	750	[28]
Highsurface-area g-C3N4	290	550	[32]
MIL-101(Cr)	388.7 8	533.22	This work

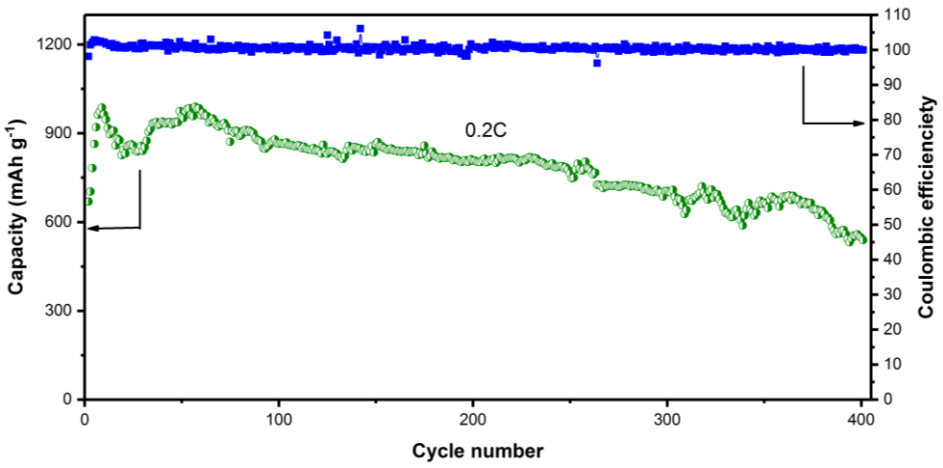

Figure 6. Cycling performance and Coulombic efficiency of the MIL-101(Cr)/S cathode at 0.2C current density for 400 cycles.

The MIL-101(Cr)/S cathode is tested at different current densities to study the rate capability performance. As shown as Figure 5c, a specific capacity of 1210.5, 1127.6, 947.7, 390.2, and 232.3 mA h g^{-1} can be obtained at 0.1C, 0.2C, 0.5C, 1C and 2C current density, respectively. Obviously, the capacity of the MIL-101(Cr)/S cathode decreases gradually from the reversible 1210.5 mA h g^{-1}at 0.1 C to 947.7, at 1210.5 mA h g^{-1} at 0.5C. However, the capacity of the MIL-101/S cathode decreases rapidly from the 947.7 mA h g^{-1}at 0.5 C to 232.3 mA h g^{-1} at 2C. Combined with the analysis of charge-discharge capacity curves of the initial cycles, we can make a conclusion that MIL-101(Cr) as a host of sulfur can inhibit the shuttle effect of lithium polysulfides effectively, but its poor conductivity limits the charging and discharging of large currents density for Li-S batteries. The main reason maybe is that the sulfur of inside in the pores cannot be fully reaction with the higher current density. When the charge and discharge current density returned to 0.1C, the capacity can retain back to 973.6 mA h g^{-1}, showing a good rate capability at low current density.

Hundreds of cycles measurements with a fresh cell were carried out to evaluate the cycling performance of the MIL-101(Cr)/S cathode. Figure 6 displays the cycling performance of the MIL-101(Cr)/S cathode at a 0.2C current density in a voltage range of 1.7 to 2.8 V. It can be clearly seen from the figure 7 that the capacity of the first nine cycles is increasing sequentially. This is mainly due to the gradual activation of sulfur in the MIL-101(Cr) cavity. The capacity is rapidly attenuated from the 10th to the 20th cycle, and the reason of the rapid attenuation is the lithium polysulfide dissolved in the electrolyte causing the loss of active material. As the shuttle effect is suppressed by MIL-101(Cr), the capacity of a gradually increases to 996.4 mA g-1 and gradually decreases with a very small amplitude in the subsequent 345 cycles. After 400 cycles, the capacity remained at 541 mAh g^{-1}, corresponding to a capacity retention of 60.1%. The average coulombic efficiency is over 97%, showing excellent cyclic reversibility for MIL-101(Cr)/S cathode.

4. CONCLUSION

In summary, we have successfully prepared large surface area MIL-101(Cr) as a sulfur host to prepare the MIL-101(Cr)/S cathode for Li-S batteries. The microporous cage of MIL-101(Cr) has shown great ability to suppress shuttle effect of lithium polysulfides during the charge and discharge process. Thus, it has exhibited the better rate performance and cycle stability of the cathode. And it delivers a reversible capacity of 541 mAh g^{-1} after 400 cycles, and the capacity retention reaching 60.1%. If some strategies are used to improve the conductivity for MIL-101(Cr), we believe that MIL-101(Cr) will be able to better serve for long-life and high performance lithium-sulfur batteries.

ACKNOWLEDGMENTS
This work was financially supported by the National Natural Science Foundation of China (Grant No.11264023).

References

1. R. Fang, S. Zhao, Z. Sun, D.-W. Wang, H.-M. Cheng, and F. Li, *Adv. Mater.,* 29 (2017) 1606823.
2. G. Zhou, E. Paek, G. S. Hwang, and A. Manthiram, *Nat. Commun*., 6 (2015).

3. X. Ma, G. Ning, Y. Wang, X. Song, Z. Xiao, L. Hou, W. Yang, J. Gao, and Y. Li, *Electrochim. Acta,* 269 (2018) 83.
4. G. Hu, C. Xu, Z. Sun, S. Wang, H.-M. Cheng, F. Li, and W. Ren, *Adv. Mater*., 28 (2016)1603.
5. G. Zhou, J. Sun, Y. Jin, W. Chen, C. Zu, R. Zhang, Y. Qiu, J. Zhao, D. Zhuo, Y. Liu, X. Tao, W. Liu, K. Yan, H. R. Lee, and Y. Cui, *Adv. Mater*., 29 (2017) 1603366.
6. F. Pei, L. Lin, D. Ou, Z. Zheng, S. Mo, X. Fang, and N. Zheng, *Nat. Commun*., (2017) 8.
7. G. Xu, A. Kushima, J. Yuan, H. Dou, W. Xue, X. Zhang, X. Yan, and J. Li, *Energy Environ. Sci*., 10 (2017) 2544.
8. M. D. Patel, E. Cha, C. Kang, B. Gwalani, and W. Choi, *Carbon*, 118 (2017) 120.
9. Z. Zhang, L.-L. Kong, S. Liu, G.-R. Li, and X.-P. Gao, *Adv. Energy Mater.,* 7, (2017) 1602543.
10. D. Su, M. Cortie, and G. Wang, *Adv. Energy Mater.,* 7 (2017) 1602014.
11. Y. Zhong, X. Xia, S. Deng, J. Zhan, R. Fang, Y. Xia, X. Wang, Q. Zhang, and J. Tu, *Adv. Energy Mater*., 8 (2018) 1701110.
12. W. Su, *Int. J. Electrochem. Sci.,* (2018) 6005.
13. Y. Zhang, Y. Zhao, A. Yermukhambetova, Z. Bakenov, and P. Chen, *J Mater Chem A,* 1 (2013) 295.
14. G. Ai, Y. Dai, W. Mao, H. Zhao, Y. Fu, X. Song, Y. En, V. S. Battaglia, V. Srinivasan, and G. Liu, *Nano Lett*., 16 (2016) 5365.
15. X. Liang, Y. Rangom, C. Y. Kwok, Q. Pang, and L. F. Nazar, *Adv. Mater*., 29 (2017) 1603040.
16. L. Ni, G. Zhao, G. Yang, G. Niu, M. Chen, and G. Diao, ACS Appl. *Mater. Interfaces,* 9 (2017) 34793.
17. H.-J. Peng, G. Zhang, X. Chen, Z.-W. Zhang, W.-T. Xu, J.-Q. Huang, and Q. Zhang, *Angew. Chem. Int. Ed*. 55 (2016) 12990.
18. Z. Yuan, H.-J. Peng, T.-Z. Hou, J.-Q. Huang, C.-M. Chen, D.-W. Wang, X.-B. Cheng, F. Wei, and Q. Zhang, *Nano Lett.,* 16 (2016) 519.
19. H. Furukawa, K. E. Cordova, M. O'Keeffe, and O. M. Yaghi, *Science,* 341 (2013) 1230444.
20. Z. Li, C. Li, X. Ge, J. Ma, Z. Zhang, Q. Li, C. Wang, and L. Yin, *Nano Energy,* 23 (2016) 15.
21. Z. Wang, X. Li, Y. Cui, Y. Yang, H. Pan, Z. Wang, C. Wu, B. Chen, and G. Qian, Cryst. *Growth Des*., 13 (2013) 5116.
22. T. Wang, J. Wang, C. Zhang, Z. Yang, X. Dai, M. Cheng, and X. Hou, *The Analyst,* 140 (2015) 5308.
23. R. Demir-Cakan, M. Morcrette, F. Nouar, C. Davoisne, T. Devic, D. Gonbeau, R. Dominko, C. Serre, G. Férey, and J.-M. Tarascon, *J. Am. Chem. Soc*., 133 (2011) 16154.
24. W. Bao, Z. Zhang, Y. Qu, C. Zhou, X. Wang, J. Li, *J. Alloys Compd*., 582 (2014) 334–340.
25. G. Ferey, *Science,* 309 (2005) 2040.
26. Z. Pang, H. Tong, X. Wu, J. Zhu, X. Wang, H. Yang, Y. Qi, *Opt. Quantum Electron*. 50 (2018).
27. N. Xu, T. Qian, X. Liu, J. Liu, Y. Chen, C. Yan, *Nano Lett.,* 17 (2017) 538–543.
28. Z. Li, C. Li, X. Ge, J. Ma, Z. Zhang, Q. Li, C. Wang, L. Yin, *Nano Energy,* 23 (2016) 15–26.
29. X. Liang, M. Zhang, M. R. Kaiser, X. Gao, K. Konstantinov, R. Tandiono, Z. Wang, H.-K. Liu, S.-X. Dou, and J. Wang, *Nano Energy,* 11 (2015) 587.
30. Y. Li, J. Fan, J. Zhang, J. Yang, R. Yuan, J. Chang, M. Zheng, Q. Dong, *ACS Nano,* 11 (2017) 11417–11424.
31. Z. Li, S. Deng, R. Xu, L. Wei, X. Su, M. Wu, *Electrochimica Acta*, 252 (2017) 200–207.
32. Q. Pang, L.F. Nazar, *ACS Nano,* 10 (2016) 4111–4118.